Optical Architectures for Programmable Filtering and Correlation of Microwave Signals

Daniel Dolfi, Jérôme Tabourel, Olivier Durand, Vincent Laude, Jean-Pierre Huignard, *Senior Member, IEEE,* and J. Chazelas

***Abstract*— New optoelectronic architectures are presented, based on parallel delay lines, performing programmable filtering of microwave signals. According to current performances of optoelectronic components, they can process optically carried microwave signals over frequency bandwidths as large as 20 GHz, with a time-frequency product up to 10^3. The operating principle of these structures is detailed and followed by the preliminary experimental demonstration at 1.3 GHz of a 53-dB rejection filter.**

***Index Terms*—Microwave-signal processing, optics.**

I. Introduction

THE availability of optoelectronic components operating in the multigigahertz domain (up to 20 GHz) brings attractive perspectives for optical processing of microwave signals [1]–[14]. Owing to their inherent parallel-processing capabilities, optoelectronic architectures are well suited for the implementation, in radar and electronic warfare (EW) systems, of basic functions such as spectrum analysis, adaptive filtering, and correlation. Furthermore, optically carried microwave signals can experience large time delays, especially in fiber-based systems, providing time–frequency products in the range between 10^2–10^4. These potential performances are very attractive for radar imaging, stealth target detection, jammers localization, and excision. In this paper, the authors propose, and experimentally demonstrate, a new optoelectronic programmable filter in which time delays are generated by a diffractive mirror (DM) and parallel weighting is obtained with a liquid crystal spatial light modulator (LCSLM).

II. Transversal Filtering

A transversal filter optimizes the detection in a signal $x(t) = S(t) + N(t)$ of a given signal $S(t)$, with duration T, in presence of a stationary noise $N(t)$, or permits jammers rejection from detected signals. Matched filtering is a particular case which maximizes the signal-to-noise ratio in presence of a white noise. The output $y(t_0)$ of this filter at time t_0 is expressed by

$$y(t_0) = \int_{t_0-T}^{t_0} x(t)S(t-t_0)\,dt. \tag{1}$$

These signals are often processed in a sampled form using a delay line made with n coupling elements separated by time delay τ_i and providing the samples $x(t)\cdots x(t-k\tau_i)\cdots x(t-n\tau_i)$. Each of these samples can be weighted with a normalized weight α_k to provide the output $\alpha_k \cdot x(t-k\tau_i)$ where α_k is given by: $\alpha_k = S[(n-k)\tau_i]/|S_{\max}|$. $S_{\max}$ is the maximum value of $S(t)$ over time duration T. In this case, (1) becomes a discrete sum of products and matched filtering reduces to a *weighting* method. If one sums these $(n+1)$ weighted outputs at time t_0, one obtains, after the following change of coordinates $T = n\tau_i$ and $t_0 - k\tau_i = t_k$, a term proportional to

$$\sum_{k=0}^{n} x(t_k)S[t_k - (t_0 - T)]. \tag{2}$$

Compared to (1), this term appears as the sampled output $y_s(t_0 - T)$ of the matched filter at time $t_0 - T$. The time delay τ_i represents the sampling period, and $B = 1/2\tau_i$ is the processed frequency bandwidth. Digital electronic delay lines allows one to process signals with a rather large number of sampling points (up to 10^2–10^3), but with a frequency bandwidth B limited to the low and intermediate frequencies (100 MHz–1 GHz) [11]. Therefore, processing of the whole 20-GHz bandwidth is not possible, and is done successively over intervals of a few gigahertz. On the other hand, optical-fiber delay lines present the advantage to process signals over a large frequency bandwidth, but they are generally implemented with a reduced number of sampling points (10–100) [2]–[9], and the weighting is difficult to obtain. Therefore, an optical architecture of a programmable filter is proposed, which could provide a large number of samples of about 10^3, and which may process signals over a frequency bandwidth as large as 20 GHz.

III. Optical Architecture

The operating principle of this programmable filter, recently reported in [15], is shown in Fig. 1. A continuous-wave (CW) laser diode of wavelength λ is coupled into an integrated optic-amplitude modulator, excited by a signal $x(t)$, in the microwave range. The outcoming beam is then an optical carrier of this signal $x(t)$. It is expanded and reflects off a DM, which operates in the Littrow geometry, i.e., in a geometry

Manuscript received December 12, 1996; revised April 25, 1997.

D. Dolfi, J. Tabourel, O. Durand, V. Laude, and J.-P. Huignard are with Thomson-CSF, Laboratoire Central de Recherches, 91404 Orsay Cedex, France.

J. Chazelas is with Thomson-CSF, Radars et Contre-Mesures, 78852 Elancourt Cedex, France.

Publisher Item Identifier S 0018-9480(97)06015-8.

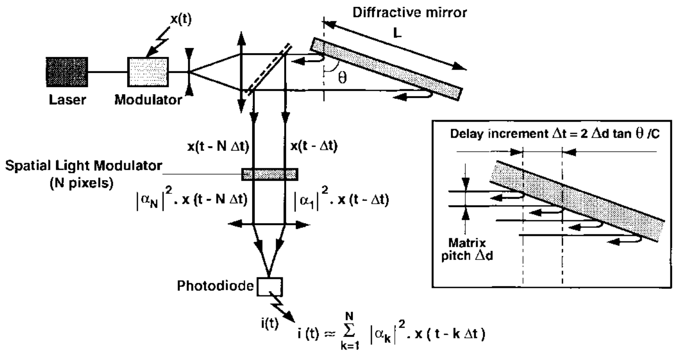

Fig. 1. Operating principle of the programmable filter: L = length of the DM, θ = angle of incidence of the plane wave.

where the diffracted beam is retroreflected. It is, for instance, a classical blazed grating or, as proposed in [16], a Bragg grating recorded in a photopolymer material. This reflected beam, extracted with a beam-splitter, passes through a one-dimensional (1-D) spatial light modulator (SLM) of N pixels, which can be for instance, a liquid crystal SLM. Finally, the channelized beam is focused onto a photodiode. According to the operating principle of the DM, the elementary incident plane waves, which diffract on two successive steps of the grating, undergo an elementary path–length difference of λ, corresponding [for the carried signal $x(t)$] to an elementary time delay of λ/c (c = velocity of light). Therefore, the incident plane wave which diffracts on the mirror aperture undergoes a maximum path–length difference of $2L\sin\theta$ (see Fig. 1) corresponding to a maximum time delay $T = 2L\sin\theta/c$. The pixels of the SLM have a center-to-center spacing Δd and provide, via a control voltage, a weighting of the amplitude of the light with coefficients α_k.

Since the DM diffracts a plane wave ($k \cdot \omega \cdot \Delta t/2\pi$ is an integer and $\Delta t = 2 \cdot \Delta d \cdot \tan\theta/c$ is the delay increment), every k channel of the SLM transmits an optical field E_k, which is expressed for a low modulation ratio m by

$$E_k = \alpha_k \cdot E_0 \cdot [1 + j \cdot \exp \mathrm{j} \cdot (\mathrm{m} \cdot \mathrm{x}(\mathrm{t} - \mathrm{k}\Delta\mathrm{t}))] \cdot \exp[\mathrm{j}(\omega\mathrm{t} + \phi_\mathrm{k})].$$

It is an optical carrier of the delayed signal $x(t - k\Delta t)$. E_0 is the amplitude of the optical field associated to the diffracted plane wave. In the following, the developed analysis also takes into account possible phase aberrations ϕ_k induced by the DM and the SLM.

When the coherence time t_c of the source is smaller than the increment Δt ($t_c \ll \Delta t$), i.e., with a superluminescent diode, the integration on the surface S of a detector with responsivity Γ amounts to an incoherent summation by a lens (with focal length F) of all the intensities provided by each pixel (see Fig. 1). The photodiode then delivers the photocurrent

$$\begin{aligned} i(t) &= \Gamma \int_s \left\langle \sum_{k=0}^{N} |E_k|^2 \right\rangle dS \\ &= \Gamma S |E_0|^2 \sum_{k=0}^{N} |\alpha_k|^2 |1 + j \cdot e^{jm \cdot x(t - k\Delta t)}|^2 \end{aligned} \tag{3}$$

where the notation "<>" denotes time averaging over the response time of the photodiode. It reduces, for $m \ll 1$, to

$$i(t) \approx 2\Gamma S|E_0|^2 \sum_{k=0}^{N} |\alpha_k|^2 - 2m\Gamma S |E_0|^2 \sum_{k=0}^{N} |\alpha_k|^2 \cdot x(t - k\Delta t). \tag{4}$$

The first term in (4) is a constant bias. The second one is the result of the matched filtering of the signal $S(t)$, if one chooses the coefficient α_k so that $|\alpha_k|^2 = S(T - k\Delta t)$.

If the coherence of the source is large ($t_c \gg \Delta t$) one now has to consider a coherent optical summation of all the emerging channels. When the photodiode diameter $\varnothing$ is small compared to the highest spatial frequency provided by the SLM, i.e., $\varnothing \le \lambda \cdot F/N \cdot \Delta d$, then the photocurrent is expressed by

$$i(t) = \Gamma \int_s \left\langle \left| \sum_{k=0}^{N} E_k \right|^2 \right\rangle dS \tag{5}$$

which, for $m \ll 1$ and $\phi_{kk'} = \phi_k - \phi_{k'}$, leads to

$$\begin{aligned} i(t) = {} & 2\Gamma S |E_0|^2 \sum_{k=0}^{N} |\alpha_k|^2 + 4\Gamma S |E_0|^2 \\ & \cdot \sum_{k=0}^{N} \sum_{k' \neq k} \alpha_k \cdot \alpha_{k'} \cos\phi_{\mathrm{kk'}} \\ & - 2m\Gamma S |E_0|^2 \sum_{k=0}^{N} \beta_k \cdot x(t - k\Delta t) \end{aligned} \tag{6}$$

$$\beta_k = |\alpha_k|^2 + \sum_{k' \neq k} \alpha_k \cdot \alpha_{k'} (\cos\phi_{\mathrm{kk'}} + \sin\phi_{\mathrm{kk'}}). \tag{7}$$

It corresponds to a spatial filtering, taking into account only the on-axis plane wave component. One can notice that (6) is equivalent to (4) except for supplementary terms of interference between the pixels of the SLM. First terms correspond to a continuous background. The last one is the result of matched filtering of the signal $S(t)$, if one chooses the coefficient β_k so that $\beta_k = S(T - k\Delta t)$. In this case, weighting coefficients α_k of every pixel k are deduced from (7). Note that negative weighting is then possible.

Furthermore, when the photodetector size is increased up to $\varnothing \ge \lambda \cdot F/\Delta d$ with $t_c \gg \Delta t$, then all the spatial frequencies of the image displayed onto the SLM are collected and averaged by the photodiode. In this case, the contribution of the terms $\phi_{kk'}$ vanishes and the modulated photocurrent reduces to the incoherent summation of (4).

The response time of the proposed programmable filter is mainly determined by the response time T_r of the LCSLM. Ferroelectric or chiral smectic LCSLM's exhibit switching time in the range of 10–100 μs, but with poor analog grey-scale performance. Conversely, nematic LCSLM's classically provide up to 256 grey levels, but with the drawback of response times in the range of 10–100 ms. In order to meet radar or EW systems requirements, in term of adaptive processing speed in the range of 10 ns–10 μs, it would be necessary to use multiple quantum well (MQW) SLM's [17]

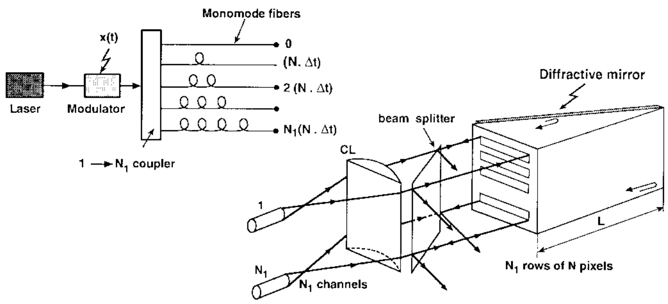

Fig. 2. Operating principle of a 2-D programmable filter for large delay values: DM provides a maximum time-delay $N \cdot \Delta t$. N_1 fibers provide time delays with a $N \cdot \Delta t$ increment. Maximum duration of the analyzed signal $T = N_1 \cdot N \cdot \Delta t$. In order to increase the time-delay values, the grating can be glued as shown onto a prism.

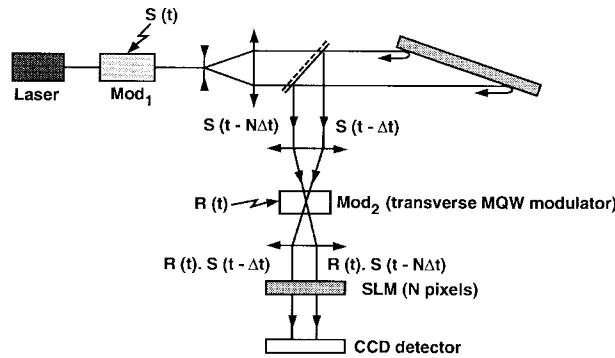

Fig. 3. Operating principle of the correlator.

or to take advantage of the high resolution of LCSLM's. Their resolution (up to $10^3 \times 10^3$) permits the extension of this concept to a two-dimensional (2-D) architecture in which a $N \times P$ pixel LCSLM provides in parallel P columns of N weightings $\alpha_{k,\,j}\,(1 \leq j \leq P,\, 1 \leq k \leq N)$. Each one of the P channelized beams is focused onto one of the photodiode of a P detector array, using for instance, a cylindric lens or a P spherical-lens array. In this case, the adaptive processing time is about T_r/P and could match system specifications for $P \approx$ 10–100.

According to the proposed 1-D optical architecture, the maximum delay value is determined by the size of the holographic mirror. Since it is not realistic to extend the size L of this mirror beyond 20 cm with an incidence angle θ exceeding 70–80°, the maximum delay $N \cdot \Delta t$, i.e., the maximum duration T of the analyzed signal, is limited to the nanosecond range. In order to overcome this limitation and to increase T up to hundreds of nanoseconds, it is possible to take advantage of the use of a high refractive-index prism in conjunction with a 2-D extension of the concept, as proposed in Fig. 2. In this case, the output of the high-speed modulator is coupled to N_1 fibers in order to get N_1 delays with an increment $N \cdot \Delta t$ equivalent to the one provided by the diffractive mirror and the prism. The output of each fiber is collimated using a cylindrical lens and illuminates (as shown in Fig. 2) a row of N pixels of a 2-D SLM with $N \times N_1$ pixels. Finally, the channelized beam is focused onto a single high-speed photodiode, providing the weighted sum of the $N \times N_1$ delayed samples, with an increment Δt, of the signal $S(t)$.

Furthermore, it is possible to combine both 2-D extensions of the concept, using a $(N \times N_1) \times P$ pixel SLM with a P photodiode array in order to provide high-speed processing and large time delays, i.e., time frequency up to 10^3–10^4.

IV. Correlator

In addition, the proposed parallel-filter achitecture can be extended to provide real-time correlation capabilities which could be exploited, for instance, in direction-finding systems. The operating principle of the correlator, in a 1-D configuration, is shown in Fig. 3. A CW laser is coupled into a first integrated-optic amplitude modulator M_1, excited by a microwave signal $S(t)$. It is expanded, using cylindrical lenses, and reflects off the DM. This reflected beam is focused through a second modulator M_2 excited by a signal $R(t)$. Since this modulator must operate in the microwave range, and preserve the different angles of incidence of the laser beam, it could be, therefore, a transverse electro-absorption MQW modulator [17], combining both high-speed operation and large angular aperture. In this case, each direction of the laser beam is then carrying a microwave signal $S(t - k \cdot \Delta t) \cdot R(t)$. The laser beam is then collimated and travel through, for instance, a 1-D LCSLM of N pixels, providing the weighting α_k. Finally, the channelized beam is detected by a CCD array with a time of integration T.

Each pixel k of the CCD array will detect a part of the beam corresponding to a delayed sample of the signal $S(t)$, and will deliver a correlation signal $C(k \cdot \Delta t)$ as follows:

$$C(k \cdot \Delta t) \propto \int_T |\alpha_k|^2 \cdot S(t - k \cdot \Delta t) \cdot R(t)\, dt. \tag{8}$$

According to the operating principle of the incoherent modulator M_2, and since the spatial summation on a single photodetector (transversal filter) is replaced by a time integration on each pixel of the CCD detector, it is no longer necessary to consider the coherence time of the laser. Furthermore, this proposed optical architecture can also benefit, as for the transversal filter of a 2-D extension in order to improve its capabilities in terms of large time delays and parallel-processing speed.

V. Implementation

As proof of this concept, a parallel filter is implemented using a CW laser diode (60 mW at 840 nm) with a large coherence time ($t_c \gg \Delta t$, $t_c \approx 0.1\ \mu$s). It is coupled through a polarization-maintaining fiber into an integrated-optic Mach–Zehnder modulator, excited by a microwave signal $x(t)$. The outcoming beam is expanded and reflects off the DM (diffraction efficiency ≈90%), which operates in a double-pass geometry (see Fig. 4). Since the DM is polarization selective, it is necessary to use a retardation plate in order to maximize the optical power of the diffracted beam. Then the beam passes through a video controlled (256 grey levels) LCSLM (320*264 pixels of area 56 × 44 μm^2 with a 80-μm matrix pitch) and is detected by a Si avalanche photodiode.

In order to verify the delays undergone by a signal $x(t)$ in the range 0.6–1.3 GHz, emerging light is detected through a

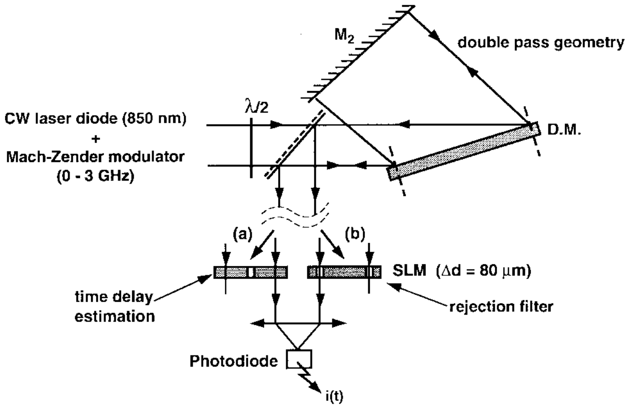

Fig. 4. Implementation of the adaptive filter: $L = 58$ mm, DM $= 1800$ lines/mm, $F = 120$ mm. In the experiment, the mirror M_2 is slightly tilted with respect to the autocollimation direction, in order to avoid the use of a beam-splitter, which is replaced by a mirror not represented here.

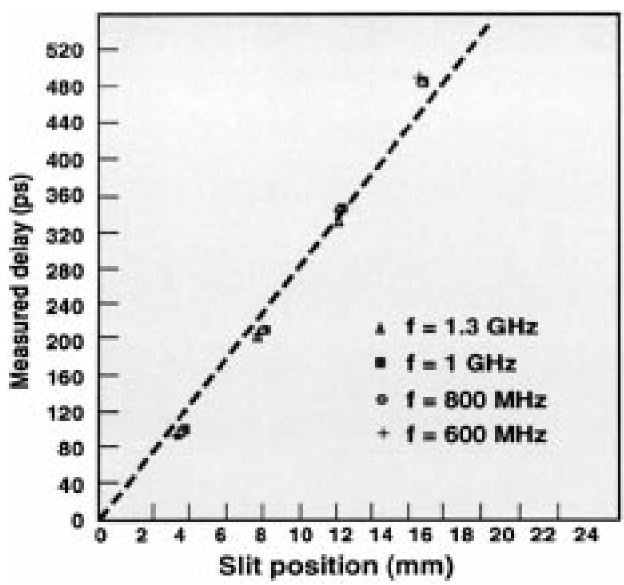

Fig. 5. Time delay experienced by the optical carrier: whatever the frequency used in the range 0.6–1.3 GHz, the delay undergone by the signal $S(t)$ across the aperture varies linearly with the position of the moving slit from one edge of the collimated beam to the other one. Maximum value ≈ 0.5 ns.

1-mm slit, which is moved across the aperture D of the beam [see Fig. 4(a)]. It shows that whatever the frequency used, the signal experiences a delay which linearly varies with the position of the slit. The maximum delay T is constant with frequency and equal to 480 ps (see Fig. 5).

As proof of this concept, the maximum delay obtained allowed one to implement a simple rejection filter over a 2-GHz bandwidth. The rejection filter is presented here only as an example. The main interest of this architecture is to perform parallel filtering with a large number of samples, maintaining a low-loss level due to free-space propagation. The modulator is fed with a microwave signal at frequency f and an image of two slits is displayed onto the SLM [see Fig. 4(b)]. They define two channels corresponding to the two edges of the DM, with the relative maximum time delay T. The diameter of the detector (80 μm) is large compared to the dimension $\lambda \cdot F/N \cdot \Delta d \approx 4$ μm ($F = 120$ mm, $N \cdot \Delta d = 25.6$ mm),

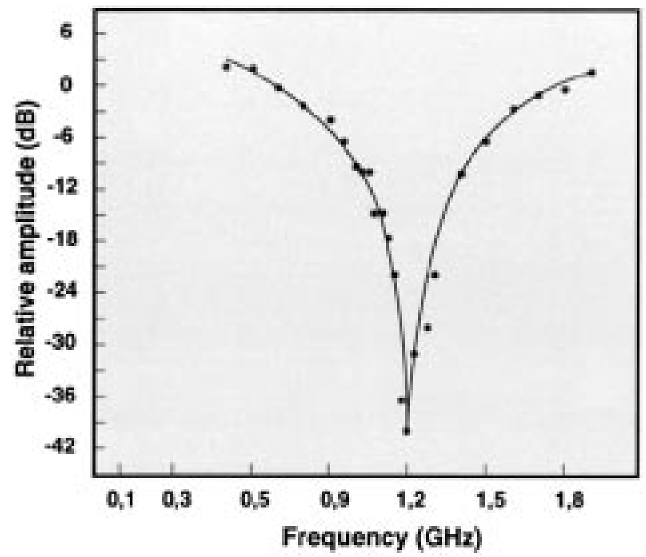

Fig. 6. Rejection filter response obtained with a two-slit figure displayed on the SLM: the relative amplitude is given by the ratio: $y_s(f, t)/y_1(f, t)$. The signal $y_1(f, t)$ corresponds to the beam transmitted by only one of the two slits.

which has to be considered here since only the two extreme pixels are taken into account. In this case, the modulated photocurrent i_m reduces to the sum of two components and is given as expressed in (4), by

$$i_m(f, t) = i_1 \cdot \cos 2\pi \mathrm{ft} + \mathrm{i}_2 \cdot \cos 2\pi \mathrm{f}(\mathrm{t} - \mathrm{T}) \qquad (9)$$

where i_1 and i_2 are the photocurrents amplitude corresponding to the detection of the signal provided by one of the two slit alone. For a given frequency f_0, corresponding to $2\pi f_0 T = \pi$, this modulated photocurrent vanishes, which means that a rejection filter canceling the frequency f_0 of the signal $x(t)$ is obtained. The power transmission (in decibels) of the synthesized filter at frequency f_0 is proportional to

$$\langle i_m^2(f) \rangle \approx 10 \log \left[\frac{1}{2}\left(1 + \cos \pi \frac{\mathrm{f}}{\mathrm{f}_0}\right) + 2\left|\frac{\mathrm{i}_1 - \mathrm{i}_2}{\mathrm{i}_1 + \mathrm{i}_2}\right|^2 \right] \qquad (10)$$

assuming second-order Taylor expansion for $|i_1 - i_2| \ll i_1, i_2$.

Therefore, with a SLM providing a contrast ratio

$$\left|\frac{i_1 - i_2}{i_1 + i_2}\right| \approx 10^{-3}$$

it is possible to implement a filter at f_0 with a rejection of about 50 dB. The measured filter response (see Fig. 6) shows a 40-dB rejection of signal $y_s(f_0, t)$ at $f_0 = 1.2$ GHz, apparently mainly limited by the long-term stability of the setup.

In order to improve this stability and to increase the microwave frequency, the parallel filter is now implemented with fiber pigtailed components operating at 1.55 μm. A fiber laser (40 mW at 1.55 μm) is coupled to an integrated-optic Mach–Zender modulator (operating up to 8 GHz, developed by Thomason-Microsonics). It is followed by an Er-doped fiber amplifier providing a 17-dB optical gain. The DM still operates in the double-pass geometry, but its size is increased up to $L = 140$ mm with a 75° incidence angle and a 48° diffraction

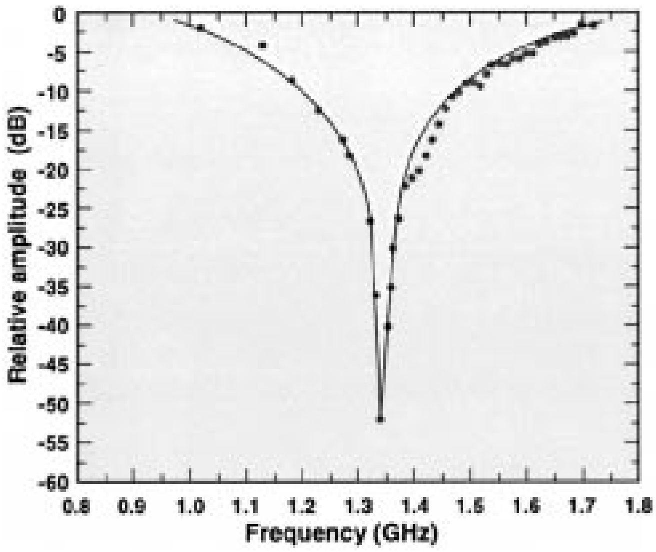

Fig. 7. Rejection filter response obtained with a two-slit figure displayed on the SLM ($\lambda = 1.55$ μm, $f_0 = 1.35$ GHz).

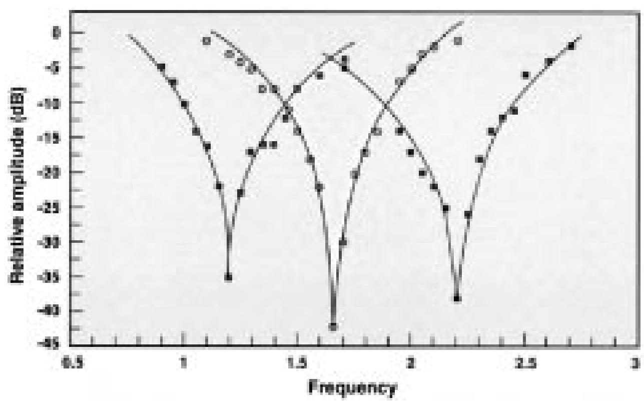

Fig. 8. Rejection filter tuning obtained with a two-slit figure with different spacings (frequency in gigahertz).

angle, providing a measured maximum delay of 750 ps. The maximum delay theoretically provided by this setup is of about 1.3 ns, but is not experienced here according to a nonoptimized illumination of the grating. Since the contrast ratio provided by the LCSLM at 1.55 μm is too small, it is replaced by a two-slit image on a slide. It provides two out-of-phase microwave signals. In these conditions, using a multimode-fiber pigtailed photodiode, it is possible to measure at 1.35 GHz at 53-dB rejection, as shown in Fig. 7.

The frequency of this filter is simply changed with the spacing between the two slits. An example of this frequency tuning, using the previously described experimental setup, is shown in Fig. 8. The width of this rejection filter is quite large since it operates almost as a microwave two-beam interferometer. Increasing the number of slits (i.e., the number of sampling points) would of course reduce by analogy with a multiple-beam interferometer, the filter width.

VI. Conclusion

To summarize, a new programmable optical architecture has been proposed, based on parallel delay lines generated by a diffractive mirror in the Littrow configuration. Channelization and weighting is provided by an SLM, and according to the exposed principle, this architecture could simultaneously process microwave signals over a frequency bandwidth as large as 20 GHz. Extensions of this concept to the implementations of a high-speed transversal filter, and to a correlator, are proposed. A 53-dB rejection filter was implemented at 1.35 GHz. According to these preliminary results, it is realistic to extend the architecture to the realization of a $N = 10^2 - 10^3$ channels filter. Performances of such an architecture in a multijammer environment, and further signal processing schemes, are investigated.

Acknowledgment

The authors would like to acknowledge P. Souchay (Thomson-CSF/Radar & Contre-Mesures) and M. Chomiki (Thomson-Microsonics) for their contributions to this paper.

References

[1] H. Zmuda and E. N. Toughlian, *Photonic Aspects of Modern Radar*. Norwood, MA: Artech House, 1994.

[2] K. P. Jackson, S. A. Newton, B. Moslehi, M. Tur, C. Chapin Cutler, J. Goodman, and H. J. Shaw, "Optical fiber delay-line signal processing," *IEEE Trans. Microwave Theory and Tech.*, vol. MTT-33, pp. 193–210, Mar. 1985.

[3] J. N. Lee, "Optical architectures for temporal signal processing," in *Optical Signal Processing*, J. L. Horner, Ed. New York: Academic, 1987, pp. 165–190.

[4] D. R. Pape, "Acousto-optic signal processors," in *Optical Signal Processing*, J. L. Horner, Ed. New York: Academic, 1987, pp. 217–240.

[5] K. B. Jackson and H. J. Shaw, "Fiber optic delay line signal processors," in *Optical Signal Processing*, J. L. Horner, Ed. New York: Academic, 1987, pp. 431–475.

[6] S. Gweon, C. E. Lee, and H. F. Taylor, "Programmable fiber optic signal processor," *IEEE Photon. Technol. Lett.*, vol. 2, pp. 382–384, May 1990.

[7] K. Sasayama, M. Okuno, and K. Habara, "Coherent optical transverse filter for 10-GHz signal processing," *Proc. topical meeting photonic switching*, Kobe, Japan, May 1990, pp. 89–91.

[8] D. Norton, S. Johns, C. Keefer, and R. Soref, "Tunable microwave filtering using high dispersion fiber time delays," *IEEE Photon. Technol. Lett.*, vol. 6, pp. 831–832, July 1994.

[9] M. Y. Frankel and R. D. Esman, "Fiber-optic tunable microwave transversal filter," *IEEE Photon. Technol. Lett.*, vol. 7, pp. 191–193, Feb. 1995.

[10] R. M. Montgomery and M. R. Lange, "Photorefractive adaptive filter structure with 40-dB interference rejection," *Appl. Opt.*, vol. 30, pp. 2844–2849, July 1991.

[11] P. M. Grant and R. S. Withers, "Recent advances in analog signal processing," *IEEE Trans. Aerospace Electron. Syst.*, vol. 26, pp. 818–849, July 1990.

[12] D. Hunter and R. Minassian, "Reflectivity tapped fibre optic transversal filter using in-fibre Bragg gratings," *Electron. Lett.*, pp. 1010–1012, 1995.

[13] D. Hunter, R. Minassian, and P. A. Krug, "Tunable optical transversal filter based on chirped gratings," *Electron. Lett.*, vol. 31, pp. 2205–2207, Dec. 1995.

[14] B. Moslehi, K. Chau, and J. Goodman, "Optical amplifiers and liquid-crystal shutters applied to electrically reconfigurable fibre optic signal processors," *Opt. Eng.*, vol. 32, pp. 974–981, May 1993.

[15] O. Durand, D. Dolfi, V. Laude, J. P. Huignard, and J. Chazelas, "Optical architecture for programmable filtering of microwave signals," *Opt. Lett.*, vol. 21, pp. 803–805, June 1996.

[16] C. Joubert, A. Delboulbé, B. Loiseaux, and J. P. Huignard, "Holographic elements for LCD projectors," *Proc. SPIE*, vol. 2406, pp. 248–259, Feb. 1995.

[17] U. Efron and G. Livescu, "Multiple quantum well SLMs" in *Spatial Light Modulators*, U. Efron, Ed. New York: Marcel Dekker, 1995, pp. 217–286.

Daniel Dolfi graduated from the Ecole Supéieure d'Optique, Orsay, Cedex, France, and received the Ph.D. degree from the University of Paris XI, Orsay, France.

He is currently a Research Scientist at Thomson-CSF Corporate Research Laboratory, Orsay, Cedex, France, where he works on optoelectronic signal processing of microwave signals, high-speed photodetectors, liquid-crystal devices, and photorefractive materials and applications.

Jérôme Tabourel received the degree in optronic engineering from the University of Paris XI, Orsay, France, in 1996.

He is currently with the R&D Department, Thomson-CSF Optronique (Guyancourt), Orsay, Cedex, France. His interests include optical limiting for optronic systems.

Olivier Durand graduated from the Ecole Nationale Supérieure des Techniques Avancées, Paris, France, in 1994, and is currently working toward the Ph.D. degree.

In 1996, he joined the R&D Department, Thomson-CSF Optronique, Orsay, Cedex, France.

Vincent Laude graduated from Ecole Supéieure d'Optique, Orsay, Cedex, France, in 1990, and received the Ph.D. degree from the University of Paris XI, Orsay, France, in 1994.

He is currently a Research Scientist at Thomson-CSF Corporate Research Laboratory, Orsay, Cedex, France. His current research interests are in optical correlation, optimal correlation filter design, optical image processing, computer-generated holograms, diffractive optics, and spatial light modulators.

Jean-Pierre Huignard (M'88–SM'89) received the engineering degree from Ecole Supéieure d'Optique, Orsay, Cedex, France, and the Ph.D. degree from the University of Paris XI, Orsay, France.

He is currently Head of the Optics and Signal Processing Laboratory at Thomson-CSF Corporate Research Laboratory, Orsay, Cedex, France. His interests include optical information processing, optical phase conjugation, and electro-optic devices.

Dr. Huignard is a member of the SPIE, SFO, and a fellow of the OSA.

J. Chazelas graduated from Ecole Centrale, Paris, France, and received the Ph.D. degree in atomic and molecular physics from Paris University, Paris, France.

In 1989, he joined the Physics Group at Thomson-CSF Corporate Research Laboratory, Orsay, Cedex, France. Since 1989, he has been in charge of advanced technologies as Deputy Director of the Analog and Microwave Department, Thomson-CSF Radars et Contre-Mesures, Elancourt Cedex, France, where he is involved in the field of optoelectronics for microwave processing.